UC Davis
UC Davis Previously Published Works

Title

Direct quantification of long-term rock nitrogen inputs to temperate forest ecosystems

Permalink

Journal

ISSN

Authors

Morford, Scott L
Houlton, Benjamin Z
Dahlgren, Randy A

Publication Date

DOI

Peer reviewed

Direct quantification of long-term rock nitrogen inputs to temperate forest ecosystems

Scott L. Morford,[1,2] Benjamin Z. Houlton,[1] and Randy A. Dahlgren[1]

[1]*Department of Land, Air and Water Resources, University of California, Davis, California, 95616-8627, USA*

Abstract. Sedimentary and metasedimentary rocks contain large reservoirs of fixed nitrogen (N), but questions remain over the importance of rock N weathering inputs in terrestrial ecosystems. Here we provide direct evidence for rock N weathering (i.e., loss of N from rock) in three temperate forest sites residing on a N-rich parent material (820–1050 mg N kg⁻¹; mica schist) in the Klamath Mountains (northern California and southern Oregon), USA. Our method combines a mass balance model of element addition/depletion with a procedure for quantifying fixed N in rock minerals, enabling quantification of rock N inputs to bioavailable reservoirs in soil and regolith. Across all sites, ~37% to 48% of the initial bedrock N content has undergone long-term weathering in the soil. Combined with regional denudation estimates (sum of physical + chemical erosion), these weathering fractions translate to 1.6–10.7 kg·ha⁻¹·yr⁻¹ of rock N input to these forest ecosystems. These N input fluxes are substantial in light of estimates for atmospheric sources in these sites (4.5–7.0 kg·ha⁻¹·yr⁻¹). In addition, N depletion from rock minerals was greater than sodium, suggesting active biologically mediated weathering of growth-limiting nutrients compared to nonessential elements. These results point to regional tectonics, biologically mediated weathering effects, and rock N chemistry in shaping the magnitude of rock N inputs to the forest ecosystems examined.

Key words: carbon nitrogen ratios; fixed ammonium; Klamath Mountains; mycorrhiza; nitrogen cycle; nitrogen isotopes; nutrient limitation; soil; tectonics; temperate forest.

Introduction

Models of the N cycle identify biological N fixation (BNF) and atmospheric deposition as the primary N inputs to terrestrial ecosystems (Delwiche 1970, Vitousek et al. 1997, Fowler et al. 2013). Nitrogen is common among sedimentary and metasedimentary rocks (Bebout et al. 2013), but questions remain over the extent to which rock weathering contributes to net N inputs in ecosystems (Schuur 2011, Ciais et al. 2013). Rocks have been implicated in high N accumulation rates in soils (Dahlgren 1994, Dixon et al. 2012), streams (Holloway et al. 1998, Montross et al. 2013), groundwater (Strathouse et al. 1980, Hendry et al. 1984), and plant pools (Cornwell and Stone 1968, Morford et al. 2011); however, these conclusions have been more correlative than direct, relying on comparisons of N-rich bedrock to measured N pools in biota, soils, and natural waters as opposed to directly quantifying the depletion of rock N pools in the soil (Houlton and Morford 2015). Here we present a new method to directly quantify in situ weathering

of rock N that can be used to improve estimates of rock N inputs to ecosystems.

Several broad factors could help to explain the occurrence and importance of rock N inputs to terrestrial ecosystems. First, the N content of bedrock parent material is an important first-order constraint, as rock N concentrations vary substantially and the distribution of N-rich parent materials is poorly constrained (Holloway and Dahlgren 2002). Sedimentary rocks harbor large reservoirs of N, attributable primarily to burial of organic matter in marine sediments (Berner 1982). Fine-grained sedimentary rocks cover ~30% of the terrestrial land surface (Suchet et al. 2003, Dürr et al. 2005), and have estimated average N concentrations between 600 and 1000 mg kg⁻¹ (Table 1). Coarse-grained sedimentary rocks and carbonates together cover ~40% of the land surface, and have lower average N concentrations (200–400 mg N kg⁻¹). Igneous rocks generally have low N content (<100 mg N kg⁻¹), while metamorphic rocks have a more variable N content depending on the N content of source rock and thermal environment during metamorphism (Boudou et al. 2008).

A second factor involves landscape erosion, which has been implicated in rock-derived inputs of cations and P in ecosystems (Vitousek et al. 2003, Porder et al. 2007). At both large and small scales, chemical

Table 1. Estimates for rock N concentration (mg kg^{-1}) by rock type.

	Rock type					
Reference	Fine-grained sedimentary	Coarse-grained sedimentary	Carbonates	Siliceous	Igneous	Metamorphic (high grade)
Li (1991)	(600–1000)	…	…	…	…	…
Wedepohl (1995)	…	…	…	…	60[‡]	…
Holloway and Dahlgren (2002)	(113–14 000)	(17–1947)	(20–7000)	(0–100)	(0–250)	(13–422)
Kerrich et al. (2006)	(73–9300)	…	…	…	…	(20–800)
Goldblatt et al. (2009)	700	250	100	…	35	250
Johansson et al. (2012)	(0–7900)[†]	…	(23–2400)	(62–1997)	…	…
Morford (2014)	698 (0–7152)	271 (57–3680)	300 (45–1910)	157 (53–1792)	80 (0–280)	148 (41–35 390)

Notes: Average values are presented where available, and value ranges (minimum–maximum) are presented in parentheses. Fine-grained sedimentary rock types include: mudstone, shale, argillite, slate, phyllite, mica-schist. Coarse-grained sedimentary include: conglomerate, sandstone, graywacke, quartzite. Estimates from the Sedimentary Geochemical Database (SedDB; Johansson et al. 2012) are reported only for values from >100 m below sea floor. Values from Morford (2014) are derived from 968 rock samples analyzed in the Pacific Southwest, USA. Ellipses indicate that no data was available for that rock type.
[†] SedDB estimates for bulk siliciclastic deposits (i.e., coarse- and fine-grained sediments combined, median value was 900 mg N kg^{-1}.
[‡] Represents average value of upper continental crust, including 14% sedimentary rocks by mass.

weathering fluxes correlate with erosion rates (Stallard and Edmond 1983, Riebe et al. 2004). These chemical fluxes are further modulated by climatic controls (White and Blum 1995), and climatic factors are particularly important among rapidly eroding landscapes where the residence time of soils and regolith are short (West et al. 2005). Ecosystems with high erosion rates but low rock N content may host higher rock N input rates than slowly eroding landscapes with high rock N content. Conversely, landscapes hosting both high rock N content and rapid erosion rates will likely support the highest rates of rock N inputs, contingent on climatic factors.

Finally, biology plays an important role in rock-weathering rates, though this factor is yet to be examined in many ecosystem settings. Generally, biological processes are thought to increase long-term bulk weathering rates through increasing soil acidity, chelating agents, and reactive mineral surface area (Drever 1994). In addition, organisms can directly target nutrient-rich minerals in soil and rock (e.g., mineral tunneling by ectomycorrhiza; Jongmans et al. 1997), suggesting that biological demand strongly regulates chemical weathering rates, particularly for minerals containing biologically important nutrients.

In this study, we present a new method to directly quantify the loss of N from bedrock, which is fundamental to understanding the factors that alter patterns of rock N input fluxes into ecosystems. Our method distinguishes between N found in pedogenic soil reservoirs (i.e., N in soil organic matter and exchangeable ionic species) vs. mineral associated N (i.e., residual rock N and clay-fixed N), and directly quantifies the net chemical mass transfer of N from mineral to biologically available reservoirs. Combined with other measures, this method allows for direct estimation of the long-term N input flux from rock to bioavailable pools at the earth surface.

We tested our new method across three forested ecosystems in the Klamath Mountains, USA. At each of these sites, we quantified the removal of N from bedrock and estimated the chemical weathering input flux of N into the ecosystem. Our study design did not provide a systematic array of biological, climate, or parent material controls; rather, each site was influenced by a combination of these factors, and our aim was to evaluate the integrative effect of physical and biological controls by estimating N inputs fluxes. In addition, we compared the weathering of N to that of the nonessential element Na$^+$ to draw further inferences on rock N weathering controls. We hypothesized that there was net N removal from bedrock minerals during soil production (H1); and the relative depletion of Na$^+$ from parent materials should have exceeded that of N (H2). Confirmation of H2 would suggest that climate-driven geochemical kinetics were the primary driver of rock N weathering at these sites, while rejection of this hypothesis would suggest biological control. Finally, we coupled our measurements to regional erosion/denudation data to estimate the rock N input to our study sites, and to contrast rock N inputs with estimates of atmospheric N inputs.

METHODS

Study sites

We investigated three sites (Colebrook, Condrey, South Fork) in the Klamath Mountain region of northern California and southern Oregon, USA (Table 2; Appendix S1: Fig. S11). Regionally, bedrock

Table 2. Site characteristics for the three sampling locations (Colebrook, Condrey, South Fork) across the Klamath Mountains in northern California and southern Oregon, USA.

Characteristic	Site		
	Condrey	South Fork	Colebrooke
Local slope (%)	14–19	13–16	10–16
Watershed slope (%)	36–40	27–33	28–30
Relief (m)	880–1180	1052–1080	760–1130
Watershed area (km^2)	4.9–11.2	10.9–12.3	7.8–13.4
Mean annual temperature (°C)	6	9	8
Mean annual precipitation (mm)	1000	1520	3600
Rock N (mg kg^{-1})	840–862	821–1052	867–1018
Soil residence time (kyr)	3.0–5.0	0.9–2.2	2.5–4.5
Soil taxonomy	dystroxerept	dystroxerept	dystrudepts
Latitude, longitude (°N, °W)[†]	41.93, 122.98	40.29, 123.29	42.47, 124.16

[†] Based on the WGS84 (World Geodetic System).

is derived from Paleozoic and Mesozoic accreted island arc terranes stitched together by coeval volcanic-plutonic rocks (Snoke and Barnes 2006). Modern uplift rates throughout this region range from 1 to 4 mm yr^{-1} (Merritts and Bull 1989), and denudation rates range from 0.2 to 1.25 mm yr^{-1} (Balco et al. 2013). Uplift and denudation rates increase from north to south across the region, with the highest rates found in landscapes inland from Cape Mendocino and the Mendocino triple-junction.

The three sites occur on mica schist bedrock, a metasedimentary rock derived from fine-grained ocean sediments (i.e., shales, mudstones). Bedrock mineralogy is similar across sites and is dominated by an assemblage of quartz, albite, chlorite, and muscovite/sericite (Lanphere et al. 1978, Brown and Blake 1987). Nitrogen in the mica schist bedrock is found solely as NH_4^+-N, as we determined by hydrofluoric/hydrochloric acid digestion (Bremner 1959), followed by colorimetric determination (Weatherburn 1967). The three sites host different precipitation regimes (Table 2), ranging from roughly 1000 mm at Condrey to 3600 mm at Colebrooke. Both the South Fork and Condrey sites have a xeric soil moisture regime, with most precipitation occurring as snow during winter months. In contrast, the Colebrooke site has an udic soil moisture regime (bordering on xeric), and receives most of its precipitation as rain. Dominant overstory vegetation varied with climate and included *Abies magnifica*, *Abies concolor*, and *Pseudotsuga menziesii* at Condrey, South Fork, and Colebrooke, respectively.

Soils (Inceptisols) have a minimally developed B_w horizon, low base saturation (<20%, NH_4OAc method), acidic pH (pH 4.0–5.2 by 1:1 soil/water paste), and 10–18% clay in the B horizon. Depth to bedrock (R layer) is generally between 70 and 110 cm, and depth to C/Cr (saprolite) generally ranges from 50 to 60 cm. Slopes at our sampling sites ranged from 10% to 17%, but the catchment averaged slope was substantially larger, ranging from 28% to 50%.

Sampling approach

At each of the three study sites, three sampling plots were identified at convex shoulder positions in bedrock residuum/colluvium. Within each plot, three 1 × 1 m pits were excavated to hard bedrock. Soil cores were collected incrementally at 10-cm intervals from the top of the mineral horizon to hard bedrock for geochemical and bulk density analysis. At each plot, 6–9 fresh parent material samples were taken from bedrock outcrops in close proximity to the soil sampling pits.

Soils were oven dried at 110°C for 1 week and then weighed. Soils were sieved to quantify the coarse (>2 mm) and fine (<2 mm) fractions. Each soil fraction was pulverized on a SPEX SamplePrep shatterbox using a hardened-steel grinding dish for 2 minutes to pass a 74-µm sieve. N contamination from the grinding dish was evaluated by pulverizing high-purity quartz sand for 2, 4, and 6 min; all of which were below detection for N (~20 mg kg^{-1}).

Bedrock samples were cut using a slab saw to remove any weathering rind and then treated with hot 5% hydrogen peroxide to remove any surficial organic matter. A hydraulic press was used to crush rock fragments to <10 mm diameter. Rock fragments were washed with deionized water and dried at 110°C for 48 h. A 60-g subsample was then pulverized using the shatterbox method mentioned in the paragraph above.

Quantifying geologic N reservoirs in rock and soil

We used a potassium hypobromite (KOBr) digestion (Silva and Bremner 1966) to quantify pedogenic (i.e., exchangeable ionic N and soil organic nitrogen) and fixed NH_4^+ (i.e., non-exchangeable N within minerals) reservoirs in soil. The digestion procedure removes the pedogenic fraction. Following the KOBr digestion, the residual fixed NH_4^+ was quantified using a combustion elemental analyzer. The method does not distinguish between fixed NH_4^+ in primary (bedrock) minerals vs. NH_4^+ in 2:1 clay minerals. Ammonium in clay minerals may include residual N from bedrock, atmospherically derived N, or rock-derived N that was released but subsequently fixed back into minerals. Thus, our approach represents the net exchange of NH_4^+ between minerals and ecosystem pools in our

mass balance calculations, and may underestimate the amount of rock N that has become bioavailable in soil. The fixed NH_4^+ (N_{fix}) concentration in each sample was calculated using the mass of the digested (M_{dig}) and undigested samples (M_{bulk}) as follows:

$$N_{fix} = N_{dig} \frac{M_{dig}}{M_{bulk}}. \tag{1}$$

The pedogenic soil reservoir (N_{ped}) was then calculated by difference using total N (N_{tot}) and N_{fix}:

$$N_{ped} = N_{tot} - N_{fix}. \tag{2}$$

We used a Vario EL cube elemental analyzer (Elementar Americas, Mount Laurel, New Jersey, USA) with an oven temperature of 1050°C (combustion temperature of 1800°C) to quantify total (bulk and soil N) and residual N (hypobromite digested soil, N_{dig}). The detection limit for our samples was 20 mg N kg^{-1}, with an average relative standard deviation (RSD) of 11.2% for rocks and soil <200 mg N kg^{-1}, and <3.0% for rocks and soil >200 mg N kg^{-1}. Measurements (n = 33) of the B2152 sediment standard (Elemental MicroAnalysis, Devon, UK) averaged 1071 ± 17 mg N kg^{-1} (accepted = 1020 ± 100 mg N kg^{-1}). Detailed information on the application and validation of the digestion method can be found in Appendix S2.

Soil nitrogen mass balance calculations

To calculate the weathering and net removal of fixed N from bedrock, we employed a set of classic soil-weathering mass balance models (Brimhall and Dietrich 1987, Chadwick et al. 1990, Egli and Fitze 2000). Analysis of bulk geochemistry in soils and rock was performed by ICP-OES following a lithium metaborate fusion by Acme Lab (Vancouver, Canada). Total and fixed N concentrations in soil and rock samples were determined by KOBr digestion. Soil fine (<2 mm) and coarse (>2 mm) fractions were analyzed separately, and then combined according to their fractional mass contribution to calculate changes in bulk soil. In this section, we present the system of equations and the basic rationale for our conservation of mass approach. We provide additional discussion and a full derivation of the equations in Appendix S3, and Table 3 summarizes the variables and units used in the model.

Application of mass conservation equations in soil is challenging because the volumetric relationship between a unit of soil and the bedrock it is derived from cannot be directly measured. A unit of bedrock can either increase or decrease in volume as it becomes soil. Increases in volume (dilation) arise from additions of organic matter, hydration of minerals, and biological mixing. Conversely, decreases in volume (collapse) occur due to losses of soluble and volatile elements followed by compaction by overlying soil/regolith (Appendix S3: Fig. S3).

However, volumetric changes to the rock–soil unit can be calculated in a closed geochemical system by using high field strength elements (HFSEs) that are neither lost due to leaching nor gained from atmospheric inputs. Here we used zirconium (Zr) as our closed-system (immobile) element. We evaluated this assumption by incorporating the uncertainty in geochemical measurements into our model and testing

Table 3. Variables and units used in mass balance calculations.

Variable	Units	Description
ρ_p	Mass × length^{-3}	Density of bedrock parent material
ρ_w	Mass × length^{-3}	Density of soil and/or regolith
$C_{N,p}$	Unitless (mass$_N$ × mass$_{sample}^{-1}$)	Concentration of N in bedrock parent material
$C_{Zr,p}$	Unitless (mass$_{Zr}$ × mass$_{sample}^{-1}$)	Concentration of immobile element Zr in bedrock parent material
$C_{Zr,w}$	Unitless (mass$_{Zr}$ × mass$_{sample}^{-1}$)	Concentration of immobile element Zr in soil and/or regolith
$C_{Nfix,w}$	Unitless (mass$_{Nfixed}$ × mass$_{sample}^{-1}$)	Concentration of mineral fixed N in soil and/or regolith
ε	Unitless (length^3 × length^{-3})	Deformational strain
τ_N	Unitless (mass × mass^{-1})	Mass transfer coefficient for N
k	Unitless	Index of soil samples within a single profile
l	Length	Length (z direction) of soil and/or regolith sample
M_N	Mass × length^{-2}	Mass flux of rock N per unit area from soil
PM_N	Mass × length^{-2}	Initial mass of N in soil and/or regolith profile per unit area
CDF_N	Unitless (mass × mass^{-1})	Chemical depletion fraction of bedrock N in soil/regolith relative to bedrock
D	Length × time^{-1}	Denudation rate
W_N	Mass · length^{-2} · time^{-1}	Nitrogen chemical weathering flux from bedrock

our assumption of Zr immobility against other putative immobile elements.

The deformational change in bedrock volume as it is transformed into soil is termed strain (ε). The mass of an immobile element does not change between a volume of soil and the volume of rock it is derived from, and therefore can be used to quantify volumetric changes as the rock–soil system evolves. Here we calculated ε as a function of bulk density in parent material (ρ_p) and soil (ρ_w), and concentrations of Zr in rock and soil ($C_{Zr,p}$ and $C_{Zr,w}$, respectively) as

$$\varepsilon = \frac{\rho_p C_{Zr,p}}{\rho_w C_{Zr,w}} - 1. \tag{3}$$

We also evaluated the net fractional loss of mineral-fixed NH_4^+ in each soil sample (τ_N) by using the ratio of immobile Zr to N in soils and bedrock. If rock N is chemically weathered, then the ratio of N_{fix} to immobile Zr in soil should be smaller than the ratio of N to Zr in bedrock. Full derivation of τ_N is shown in the ESM. Here, $C_{Nfix,w}$ represents N_{fix} as it is defined in Eq. 1, and represents the residual mineral-fixed NH_4^+ in a soil sample following removal of soil organic N by hypobromite digestion. Negative τ_N values represent a net release of N from bedrock into bioavailable soil pools, while positive τ_N values would indicate net N incorporation into soil (clay) minerals:

$$\tau_N = \frac{C_{Zr,p}}{C_{Zr,w}} \frac{C_{Nfix,w}}{C_{N,p}} - 1. \tag{4}$$

Next, we quantified the mass removal of N from rock over the entirety of the soil profile (M_N). Calculating M_N requires simultaneous accounting for volumetric changes in soil relative to bedrock (ε) and fractional change in the abundance of rock N in soil (τ_N). As both ε and τ_N change with soil depth, we numerically integrate over the whole soil profile to estimate a profile (or pedon) averaged mass flux. In our calculation we introduce variable l, the length of the soil sample, which accounts for potential differences in the soil sample volume when sampling by soil horizon, and also allows for calculating M_N on an area, rather than volume, basis. Further, we indexed each soil sample using k to facilitate numerical integration over the entire soil profile:

$$M_N = \rho_p C_{N,p} \sum_{k=1}^{n} \frac{\tau_{N,k}}{(\varepsilon_k + 1)} (l_k). \tag{5}$$

Additionally, we calculated the initial in situ parent material N mass (PM_N) for each soil profile. The calculation for PM_N is similar to M_N (Eq. 5), with the exception that we do not account for the

fractional depletion of rock N (τ_N) over the soil profile:

$$PM_N = \rho_p C_{N,p} \sum_{k=1}^{n} \frac{1}{\varepsilon_k + 1} (l_k). \tag{6}$$

Finally, we calculated a whole profile chemical depletion fraction (Riebe et al. 2003) for N (CDF_N), simultaneously accounting for total N removal from rock and volumetric changes between rock and soil within the entire profile:

$$CDF_N = -\frac{M_N}{PM_N}. \tag{7}$$

These mass balance equations are generalizable to other elements by replacing the $C_{Nfix,w}$ and $C_{N,p}$ variables with bulk concentrations of other elements per standard convention. Finally, while τ_j and CDF_j values are often used interchangeably (i.e., $CDF_j = -\tau_j$), CDF_N in our calculations account for changes in ε with soil depth, while pit averaged τ_N does not.

Mass balance assumptions

Our mass balance approach assumes that Zr is immobile within soil. To test this assumption, we investigated the relative mobility of Zr and titanium (TiO_2) in our samples, as the fixed relative abundance of two high field strength elements (HFSEs, here Ti and Zr) is commonly used as in indication of element immobility. We calculated $^\tau TiO_2$ using Zr as the immobile element, and rejected soil pits from our plot and site calculations if the pit-integrated $^\tau TiO_2$ was greater than the absolute value of 0.1. Next, to test the sensitivity of our immobility assumption, we calculated τ_N using both TiO_2 and Zr as the immobile element and compared the variance in τ_N attributable to assumptions of element immobility to variance attributable to analytical error and field variability. We concede that our assumption validation method is imperfect: HFSEs may be mobilized via colloidal transport without a change in their relative abundance in soil (Bern et al. 2011). However, given the relative immaturity of our soils (e.g., no evidence for transported/illuvial clay), we believe this likelihood is low.

Error propagation and uncertainty analysis

A Monte Carlo method (10 000 simulations per calculation) was used in the mass balance calculations to propagate variance attributable to analytical error and natural variability in rock parent material. We assumed these variances were normally distributed. Directly quantifying the uncertainty of soil bulk density (ρ_w) is impossible (i.e., destructive sampling with a sample size of one), so variance attributable to sample ρ_w values were estimated using a random uniform distribution of $\rho_w \pm 0.05$ g cm^{-3}.

Table 4. Chemical reservoirs and fluxes among sites.

Reservoirs and fluxes	Site					
	Condrey		South Fork		Colebrooke	
	Median	95%CI	Median	95%CI	Median	95%CI
Measured N reservoirs in soil						
N_{tot}	13.7	13.3 to 14.0	11.6	11.2 to 12.1	10.8	10.5 to 11.1
N_{ped}	5.7	5.3 to 6.1	6.5	6.1 to 6.8	5.8	5.5 to 6.0
N_{fix}	7.0	6.6 to 7.6	5.3	4.7 to 5.8	4.8	4.3 to 5.2
Modeled reservoirs/fluxes						
τ_K	−0.29	−0.31 to −0.27	−0.25	−0.30 to −0.18	−0.31	−0.37 to −0.26
τ_N	−0.37	−0.41 to −0.34	−0.48	−0.50 to −0.43	−0.49	−0.55 to −0.43
τ_{Na2O}	−0.29	−0.36 to −0.23	−0.33	−0.39 to −0.27	−0.44	−0.48 to −0.41
τ_{TiO2}	0.00	−0.03 to 0.02	−0.01	−0.10 to 0.04	−0.05	−0.07 to −0.02
CDF_K	0.29	0.29 to 0.29	0.22	0.20 to 0.23	0.30	0.28 to 0.32
CDF_N	0.37	0.36 to 0.37	0.48	0.47 to 0.49	0.48	0.46 to 0.49
CDF_{Na2O}	0.28	0.27 to 0.28	0.32	0.30 to 0.34	0.41	0.41 to 0.42
CDF_{TiO2}	0.00	0.00 to 0.00	0.01	0.00 to 0.02	0.05	0.04 to 0.06
M_N	−4.1	−4.1 to 4.0	−4.6	−4.7 to −4.6	−5.4	−5.5 to −5.4
PM_N	10.3	10.3 to 10.3	9.2	9.1–9.2	9.0	9.0 to 9.1

Notes: All values represent median and 95% confidence interval (95%CI). Nitrogen reservoirs in Mg ha^{-1}, calculated using geochemical data and soil bulk density. Modeled reservoirs and fluxes derived from our conservation of mass equations. Abbreviations are: tot, total; ped, pedogenic; and fix, fixed. See Table 3 and *Methods* for further information.

Variance among soil pits (pedons) tends to be non-parametric (e.g., heavy tailed or logarithmic distributions). To account for this, we calculated plot and site averages using bootstrapping/resampling techniques. For plot averages, individual pedon values were simulated by Monte Carlo methods, and then pit values were resampled 10 000 times to estimate a distribution of median plot values. Similarly, simulations from each plot were resampled to generate a site estimate. In the results and ESM, we present site values as median and 95% confidence intervals that account for the integrated sample analytical error, variance among pedons and parent material, as well as plot-to-plot differences. For depth plots, we used a slice-wise aggregation algorithm (Beaudette et al. 2013) to show the median ± interquartile range (25th to 75th percentile) to highlight average trends among sites. Monte Carlo and bootstrapping simulations were performed using the core and boot packages in R (Davison and Hinkey 1997, Canty and Ripley 2014, R Development Core Team 2014).

RESULTS

Mineral fixed NH_4^+ (i.e., rock N in the soil zone) comprised 44–51% of the total N reservoir in soils across sites (Table 4). Pedogenic N dominated the total N pool among surface reservoirs (0–40 cm), but fixed NH_4^+ reservoirs were dominant or co-dominant below 40 cm (Fig. 1). The initial N content of rock parent material in soils ranged from 9.0 to 10.3 Mg ha^{-1} across our sites. Of this initial N reservoir in rock, between 4.1 and 5.4 Mg N ha^{-1} was released to soils and regolith (M_N). In contrast, the total pedogenic N reservoirs in soil (N_{ped}) varied from 5.7 to 6.5 Mg N ha^{-1} across sites (Table 4). Depth profiles of τ_N showed that weathering of N-rich rock was highest among surface soils, but that much of the N release has occurred at depth in the saprolite and regolith (Appendix S1: Fig. S2).

The fractional net chemical removal of N from rock was 0.37–0.48 across sites (CDF_N). Net chemical depletion for Na$^+$ was 0.28–0.41 (CDF_{Na}), and 0.22–0.29 for K$^+$ (CDF_K). Chemical depletion of Na (CDF_{Na}) was less than CDF_N across all three sites, but these differences were not statistically significant ($P = 0.25$, paired Wilconon signed-rank test). Chemical Depletion of K (CDF_K) was similar CDF_{Na} at the Condrey site, but was lower at the other two sites (Table 4).

Titanium was relatively immobile vs. Zr across sites, with τ_{TiO2} ranging from 0.00 to −0.05 (Table 4). One pit at the Colebrooke site exceeded our error tolerance (pit total τ_{TiO2} > 0.1). This pit had a τ_N value of 0.60 ± 7.7 and would have dramatically increased the plot median estimate for N depletion. Given that this pit exceeded our error tolerance and had a standard deviation more than an order of magnitude greater than our depletion estimate, it was excluded from the analysis. Generally, both sample and pit τ_{TiO2} showed fidelity to our immobile element assumptions (Appendix
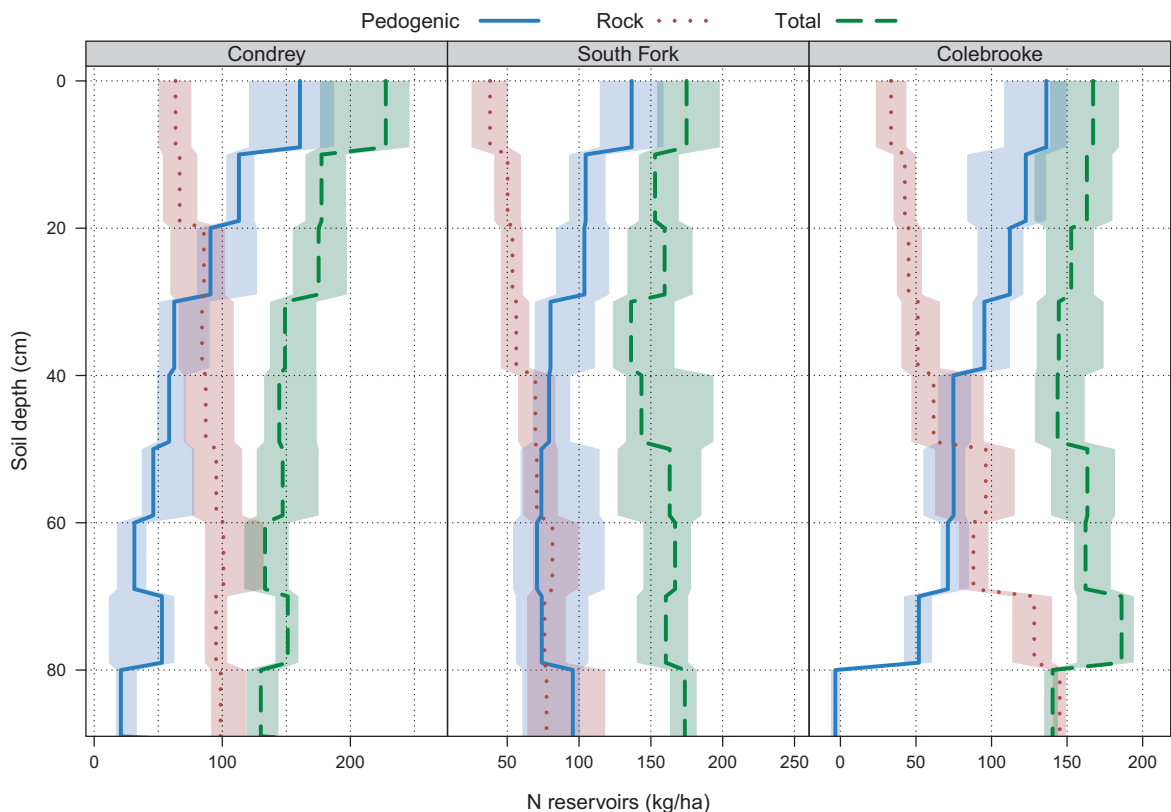
Fɪɢ. 1. Total, pedogenic, and rock (fixed-NH_4^+) nitrogen reservoirs as a function of soil depth at three sites (Colebrook, Condrey, South Fork) in the Klamath Mountain region of northern California and southern Oregon, USA. Site median (shown by solid, dotted and dashed lines) and interquartile (25th–75th percentile; shown with shaded area around lines) range reported.

S1: Fig. S3), although variance in parent material Zr and TiO_2 concentration ratios at the South Fork site did contribute to higher variance among our pit τ_{TiO2} values. Using TiO_2 as the immobile element in our calculations resulted in a < 3% change in calculated τ_N values across sites (Appendix S1: Fig. S4). These differences are less than the reported median confidence interval, indicating that Ti and Zr have similar mobility/immobility across our sites.

Pit-to-pit variance was the largest source of uncertainty in our analysis (Appendix S1: Fig. S5): For all but one plot, the uncertainty arising from analytical error plus variance in parent material geochemistry was smaller than the variance attributable to local site variability. Inter-plot variation across sites was generally smaller than the intra-plot variance, indicating that the local natural variance across landscapes is the primary driver of error and uncertainty in our mass balance calculations.

Discussion

Nitrogen depletion of in situ parent material was substantial, releasing 4.1–5.4 Mg N ha⁻¹ via chemical

weathering from rock minerals in soil (depth = 50–120 cm). These results support hypothesis one: That there is a net N removal from bedrock minerals in the forest ecosystems we studied, and contrast with investigations of NH_4^+ fixation in agricultural soils, where soil minerals have been shown to be a short-term sink (i.e., clay fixation), rather than a source, of N (Stevenson and Cole 1999). These findings suggest that NH_4^+ fixation to minerals may be substantially different between agricultural and wildland soils, perhaps due to high N fertilization among the former (Steffens and Sparks 1997, Nieder et al. 2011).

We further examined the magnitude of N inputs from parent material by utilizing long-term catchment scale denudation (D, $\sum$ physical + chemical erosion) measurements from the Klamath region (Balco et al. 2013), in combination with our chemical depletion (CDF_N) and rock N concentration ($C_{N,p}$) data. This approach allows us to constrain the in situ N chemical weathering flux (W_N) that comprises the biologically available N input to these ecosystems (Riebe et al. 2003):

(8)

$$W_N = D \cdot \rho_p \cdot C \cdot CDF_N.$$

Typically, soil weathering rates have been inferred from chemical depletion and measures of soil age at steady state (Brimhall et al. 1992); however, in actively eroding landscapes soil and surface ages cannot be directly assessed (i.e., no time zero), and instead denudation rates (D) are used to constrain mass fluxes (Riebe et al. 2001). Application of this model assumes that soil production is balanced by denudation at millennial timescales, but flux estimates are not particularly sensitive to deviations from these steady-state assumptions (Ferrier and Kirchner 2008).

We estimate that the long-term chemical weathering flux of N varies from 1.6 to 10.7 kg N·ha^{-1}·yr^{-1} in our sites (Table 5). These estimates are within the range of those observed for South Fork (3.0–10.9 kg·ha^{-1}·yr^{-1}) as based on an independent isotope-based approach (Morford et al. 2011). For comparison, long-term atmospheric N inputs (N fixation + deposition combined) for these study sites are estimated from 4.5 to 7.0 kg·ha^{-1}·yr^{-1} (Sollins et al. 1980, Cleveland et al. 1999, Dentener et al. 2006, Houlton et al. 2008). Thus, rock weathering contributes ~20–66% of total ecosystem N in these forest sites underlain by N-rich parent materials.

Integrating our rock N depletion data with denudation estimates highlights the importance of erosion rates in assessing the magnitude of rock N inputs. For example, rock N concentrations and CDF$_N$ were similar between the South Fork and Colebrooke sites, yet the rock N input for forests at South Fork were estimated to be roughly double the inputs to Colebrooke forests when integrating denudation estimates (Table 5). This demonstrates how rock N concentration and erosion need to be considered in unison when investigating long-term rock N inputs, among landscapes with moderate to high erosion rates.

We did not find evidence for higher depletion of Na vs. N from rock in these forests (H2, $P = 0.25$), although our design did not have the requisite

statistical power to detect differences among only three independent sites. However, we observed that the depletion of N from bedrock was higher than Na and K across all three forests, opposite of what standard kinetic models of mineral weathering would suggest (Goldich 1938, Brantley 2008, see Appendix S4 for further discussion). Given the mineralogy of parent materials at these sites, the more rapid depletion of N relative to other elements may be attributable to biological, rather than geochemical factors controlling the weathering of rock N at these sites. We speculate that mycorrhizal networks target N-bearing minerals, resulting in loci of enhanced weathering and N release relative to other elements, similar to mining of other biologically important elements such as Ca^{2+} in plagioclase (Jongmans et al. 1997), PO_4^- in apatite (Landeweert et al. 2001), and K^+ in biotite (Wallander 2000).

Climate also likely plays an important role in chemical weathering across our sites, but we are unable to systematically isolate climatic effects among the three sites investigated. Nevertheless, chemical depletion was generally higher in the wettest site, perhaps pointing at precipitation-driven effects in addition to lower denudation rates in driving variations in rock N inputs. This is to be expected, given the evidence of excess water as a driving factor behind chemical weathering in soil-mantled environments (Kump et al. 2000). Future work at sites that are designed to isolate precipitation as an influencing factor will be useful in understanding how climate and perhaps climate change might influence N weathering inputs to terrestrial ecosystems.

Our findings have implications for understanding N accretion in ecosystems and biological interpretation of C:N ratios derived from bulk soil measurements. First, our analysis suggests that the mechanism of N accretion in ecosystems with fresh geologic substrates harboring N is similar to accretion of other putative rock nutrients such as P and calcium (Walker and Syers 1976). The large reservoir of native reactive N found in soil parent materials in these sites (PM$_N$ = 9.0–10.3 Mg N ha^{-1}) is greater than the N reservoir found in soil organic matter (N_{ped} = 5.7–6.5 Mg N ha^{-1}), suggesting that rock-derived N could be a principal source N to organic matter as bedrock weathers to soil. However, not all of the N is removed from rock minerals during weathering at these sites (M_N = 4.1–5.4 Mg N ha^{-1}), implying that bulk C:N ratios do not solely reflect biologically mediated reservoirs (i.e., soil organic matter and recently fixed NH_4^+ in clays) at sites developing on N-rich rock. For example, at the South Fork site we previously reported bulk soil C:N ratios (0–30 cm, mol/mol) of 20.8 (Morford et al. 2011). After subtracting the contribution of residual rock N at these sites, we found that the C:N ratio of the soil organic matter pool is 29.3, similar to the C:N ratios observed for other regional forests developing on N-poor bedrock.

Table 5. Estimated long-term nitrogen fluxes across our study sites.

Model estimates	Site		
	Condrey	South Fork	Colebrooke
Rock N (mg N kg^{-1})	840–862	821–1052	867–1018
CDF$_N$	0.36–0.37	0.47–0.49	0.46–0.49
N denudation (kg N·ha^{-1}·yr^{-1})	4.5–11.4	10.9–21.7	4.6–13.5
Chemical rock N inputs (kg N·ha^{-1}·yr^{-1})	1.6–4.2	5.1–10.7	2.1–6.6
Atmospheric N inputs (kg N·ha^{-1}·yr^{-1})†	4.5–6.5	5.5–7.5	5.0–7.0
ΔN inputs (%)	25–93	68–195	30–132

† Estimate includes both biological nitrogen fixation and atmospheric deposition.

Similarly, biological interpretations of bulk soil $^{15}N/^{14}N$ may be obscured if rock and bulk soil $\delta^{15}N$ values differ. At South Fork, accounting for residual rock N did not result in a dramatic difference between bulk and organic matter $\delta^{15}N$ in soil (3.6‰ vs. 3.7‰, respectively), as rock and bulk soil values are similar. However, at the Colebrooke forest, the $\delta^{15}N$ of rock (0.25‰) and bulk soil N pools (3.1‰) differ markedly, and accounting for residual rock N indicated that the soil organic matter $\delta^{15}N$ was 5.3‰, an increase of 2.2‰ over bulk soil $\delta^{15}N$ estimates (Morford – unpublished data). Thus, using measurements of bulk soil N to infer biological processes occurring among organic reservoirs in soil may be more difficult among ecosystems harboring rock N reservoirs.

Our N mass balance investigation shows that a substantial fraction of reactive N is removed from rock via chemical weathering, constituting a large source of new, biologically available, N to these forests. These results agree with recent calls for explicit incorporation of both rock and atmospheric N inputs into modern ecosystem concepts (Houlton and Morford 2015). Rock N inputs to forest ecosystems with sedimentary parent materials could be substantial among ecosystems developing on fresh geologic substrate, particularly in montane regions with moderate to high erosion rates. The N content of the parent materials investigated here ranged between 820 and 1050 mg N kg^{-1}, which is similar to the estimates for N content of fine-grained sedimentary rocks in (600–1000 mg N kg^{-1}; Table 1). Globally, 60% of forests are developing on sedimentary and metasedimentary parent materials (Appendix S1: Fig. S6), and fine-grained sedimentary rocks contribute ~40% of the bulk parent material among these lithologies (Suchet et al. 2003). In contrast, rock N inputs are likely to be of minor importance in sites developing on N-poor bedrock (e.g., igneous rocks) and among regions developing on old, stable geomorphic surfaces where inputs of fresh bedrock are limited.

Literature Cited

Balco, G., N. Finnegan, A. Gendaszek, J. O. H. Stone, and N. Thompson. 2013. Erosional response to northward-propagation crustal thickening in the coastal ranges of the US Pacific Northwest. American Journal of Science 313:790–806.

Beaudette, D. E., P. Roudier, and A. T. O'Geen. 2013. Algorithms for quantitative pedology: a toolkit for soil scientists. Computers and Geosciences 52:258–268.

Bebout, G. E., M. L. Fogel, and P. Cartigny. 2013. Nitrogen: highly volatile yet surprisingly compatible. Elements 9:333–338.

Bern, C. R., O. A. Chadwick, A. S. Hartshorn, L. M. Khomo, and J. Chorover. 2011. A mass-balance model to separate and quantify colloidal and solute redistributions in soil. Chemical Geology 282:113–119.

Berner, R. A. 1982. Burial of organic-carbon and pyrite sulfur in the modern ocean - it geochemical and environmental significance. American Journal of Science 282:451–473.

Boudou, J. P., A. Schimmelmann, M. Ader, M. Mastalerz, M. Sebilo, and L. Gengembre. 2008. Organic nitrogen chemistry during low-grade metamorphism. Geochimica et Cosmochimica Acta 72:1199–1221.

Brantley, S. L. 2008. Kinetics of mineral dissolution. Pages 151–210 in S. L. Brantley, J. D. Kubbicki and A. F. White, editors. Kinetics of water-rock interaction. Springer, New York, New York, USA.

Bremner, J. M. 1959. Determination of fixed ammonium in soil. Journal of Agricultural Science 52:147–160.

Brimhall, G. H., and W. E. Dietrich. 1987. Constitutive mass balance relations between chemical-composition, volume, density, porosity, and strain in metasomatic hydrochemical systems: results on weathering and pedogenesis. Geochimica et Cosmochimica Acta 51:567–587.

Brimhall, G. H., O. A. Chadwick, C. J. Lewis, W. Compston, I. S. Williams, K. J. Danti, W. E. Dietrich, M. E. Power, D. Hendricks, and J. Bratt. 1992. Deformational mass-transport and invasive processes in soil evolution. Science 255:695–702.

Brown, E. H., and M. C. Blake. 1987. Correlation of early Cretaceous blueschists in Washington, Oregon and northern California. Tectonics 6:795–806.

Canty, A., and B. Ripley. 2014. boot: Bootstrap R (S-Plus) Functions. R package version 1.3-11. R Foundation for Statistical Computing, Vienna, Austria.

Chadwick, O. A., G. H. Brimhall, and D. M. Hendricks. 1990. From a black to a gray box: a mass balance interpretation of pedogenesis. Geomorphology 3:369–390.

Ciais, P., et al. 2013. Carbon and other biogeochemical cycles. Pages 465–570 in T. F. Stocker, D. Qin, G.-K. Plattner, M. Tignor, S. K. Allen, J. Boschung, A. Nauels, Y. Xia, V. Bex and P. M. Midgley, editors. Climate change 2013: the physical science basis. Contribution of Working Group I to the Fifth Assessment Report of the Intergovernmental Panel on Climate Change. Cambridge University Press, Cambridge, UK.

Cleveland, C. C., et al. 1999. Global patterns of terrestrial biological nitrogen (N-2) fixation in natural ecosystems. Global Biogeochemical Cycles 13:623–645.

Cornwell, S. M., and E. L. Stone. 1968. Availability of nitrogen to plants in acid coal mine spoils. Nature 217:768–769.

Dahlgren, R. A. 1994. Soil acidification and nitrogen saturation from weathering of ammonium-bearing rock. Nature 368:838–841.

Davison, A. C., and D. V. Hinkey. 1997. Bootstrap methods and their applications. Cambridge University Press, Cambridge, UK.

Delwiche, C. C. 1970. The nitrogen cycle. Scientific American 223:137–146.

Dentener, F., et al. 2006. Nitrogen and sulfur deposition on regional and global scales: a multimodel evaluation. Global Biogeochemical Cycles 20:GB4003.

Dixon, J. C., S. W. Campbell, and B. Durham. 2012. Geologic nitrogen and climate change in the geochemical budget of Karkevagge, Swedish Lapland. Geomorphology 167:70–76.

Drever, J. I. 1994. The effect of land plants on weathering rates of silicate minerals. Geochimica et Cosmochimica Acta 58:2325–2332.

Dürr, H. H., M. Meybeck, and S. H. Dürr. 2005. Lithologic composition of the Earth's continental surfaces derived from a new digital map emphasizing riverine material transfer. Global Biogeochemical Cycles 19:GB4S10.

Egli, M., and P. Fitze. 2000. Formulation of pedologic mass balance based on immobile elements: a revision. Soil Science 165:437–443.

Ferrier, K. L., and J. W. Kirchner. 2008. Effects of physical erosion on chemical denudation rates: a numerical modeling study of soil-mantled hillslopes. Earth and Planetary Science Letters 272:591–599.

Fowler, D., M. Coyle, U. Skiba, M. A. Sutton, J. N. Cape, S. Reis, L. J. Sheppard, A. Jenkins, B. Grizzetti, and J. N. Galloway. 2013. The global nitrogen cycle in the twenty-first century. Philosophical Transactions of the Royal Society of London B 368:20130164.

Goldblatt, C., M. W. Claire, T. M. Lenton, A. J. Matthews, A. J. Watson, and K. J. Zahnle. 2009. Nitrogen-enhanced greenhouse warming on early Earth. Nature Geoscience 2:891–896.

Goldich, S. S. 1938. A study in rock-weathering. Journal of Geology 46:17–58.

Hendry, M. J., R. G. L. McCready, and W. D. Gould. 1984. Distribution, source and evolution of nitrate in a glacial till of southern Alberta, Canada. Journal of Hydrology 70:177–198.

Holloway, J. M., and R. A. Dahlgren. 2002. Nitrogen in rock: occurrences and biogeochemical implications. Global Biogeochemical Cycles 16:1118.

Holloway, J. M., R. A. Dahlgren, B. Hansen, and W. H. Casey. 1998. Contribution of bedrock nitrogen to high nitrate concentrations in stream water. Nature 395:785–788.

Houlton, B. Z., and S. L. Morford. 2015. A new synthesis for terrestrial nitrogen inputs. Soil 1:381–397.

Houlton, B. Z., Y.-P. Wang, P. M. Vitousek, and C. B. Field. 2008. A unifying framework for dinitrogen fixation in the terrestrial biosphere. Nature 454:327–330.

Johansson, A., K. Lehnert, and L. Hsu. 2012. Status report on the SedDB Sediment Geochemistry Database. GeoPRISMS Newsletter 28:21.

Jongmans, A. G., N. van Breemen, U. Lundstrom, P. A. W. van Hees, R. D. Finlay, M. Srinivasan, T. Unestam, R. Giesler, P. A. Melkerud, and M. Olsson. 1997. Rock-eating fungi. Nature 389:682–683.

Kerrich, R., Y. Jia, C. Manikyamba, and S. M. Naqvi. 2006. Secular variations of N-isotopes in terrestrial reservoirs and ore deposits. Geological Society of America Memoir 198:81–104.

Kump, L. R., S. L. Brantley, and M. A. Arthur. 2000. Chemical, weathering, atmospheric CO_2, and climate. Annual Review of Earth and Planetary Sciences 28:611–667.

Landeweert, R., E. Hoffland, R. D. Finlay, T. W. Kuyper, and N. van Breemen. 2001. Linking plants to rocks: ectomycorrhizal fungi mobilize nutrients from minerals. Trends in Ecology and Evolution 16:248–254.

Lanphere, M. A., M. C. Blake, and W. P. Irwin. 1978. Early Cretaceous metamorphic age of the South Fork Mountain Schist in the northern Coast Ranges of California. American Journal of Science 278:798–815.

Li, Y. H. 1991. Distribution patterns of the elements in the ocean: a synthesis. Geochimica et Cosmochimica Acta 55:3223–3240.

Merritts, D., and W. B. Bull. 1989. Interpreting Quaternary uplift rates at the Mendocino Triple Junction, northern California, from uplifted marine terraces. Geology 17:1020–1024.

Montross, G. G., B. L. McGlynn, S. N. Montross, and K. K. Gardner. 2013. Nitrogen production from geochemical weathering of rocks in southwest Montana, USA. Journal of Geophysical Research-Biogeosciences 118:1068–1078.

Morford, S. L. 2014. Quantifying rock nitrogen inputs to the terrestrial biosphere. Dissertation. University of California, Davis, California, USA.

Morford, S. L., B. Z. Houlton, and R. A. Dahlgren. 2011. Increased forest ecosystem carbon and nitrogen storage from nitrogen rich bedrock. Nature 477:78–81.

Nieder, R., D. K. Benbi, and H. W. Scherer. 2011. Fixation and defixation of ammonium in soils: a review. Biology and Fertility of Soils 47:1–14.

Porder, S., P. M. Vitousek, O. A. Chadwick, C. P. Chamberlain, and G. E. Hilley. 2007. Uplift, erosion, and phosphorus limitation in terrestrial ecosystems. Ecosystems 10:158–170.

R Development Core Team. 2014. R: a language and environment for statistical computing. R Foundation for Statistical Computing, Vienna, Austria.

Riebe, C. S., J. W. Kirchner, D. E. Granger, and R. C. Finkel. 2001. Minimal climatic control on erosion rates in the Sierra Nevada, California. Geology 29:447–450.

Riebe, C. S., J. W. Kirchner, and R. C. Finkel. 2003. Long-term rates of chemical weathering and physical erosion from cosmogenic nuclides and geochemical mass balance. Geochimica et Cosmochimica Acta 67:4411–4427.

Riebe, C. S., J. W. Kirchner, and R. C. Finkel. 2004. Erosional and climatic effects on long-term chemical weathering rates in granitic landscapes spanning diverse climate regimes. Earth and Planetary Science Letters 224:547–562.

Schuur, E. A. G. 2011. Ecology: nitrogen from the deep. Nature 477:39–40.

Silva, J. A., and J. M. Bremner. 1966. Determination and isotope-ratio analysis of different forms of nitrogen in soils 5. Fixed ammonium. Soil Science Society of America Proceedings 30:587–594.

Snoke, A. W., and C. G. Barnes. 2006. The development of tectonic concepts for the Klamath Mountains province, California and Oregon. Geological Society of America Special Papers. Geological Studies in the Klamath Mountains Province, California and Oregon: A Volume in Honor of William P. Irwin. 410:1–29.

Sollins, P., C. C. Grier, F. M. McCorison, K. Cromack, and R. Fogel. 1980. The internal element cycles of an old-growth douglas-fir ecosystem in western Oregon. Ecological Monographs 50:261–285.

Stallard, R. F., and J. M. Edmond. 1983. Geochemistry of the Amazon 2. The influence of geology and weathering environment on the dissolved-load. Journal of Geophysical Research-Oceans and Atmospheres 88:9671–9688.

Steffens, D., and D. L. Sparks. 1997. Kinetics of nonexchangeable ammonium release from soils. Soil Science Society of America Journal 61:455–462.

Stevenson, F. J., and M. A. Cole. 1999. Cycles of soils: carbon, nitrogen, phosphorus, sulfur, micronutrients, Second edition. Wiley, New York, New York, USA.

Strathouse, S. M., G. Sposito, P. J. Sullivan, and L. J. Lund. 1980. Geologic nitrogen: a potential geochemical hazard in the San-Joaquin Valley, California. Journal of Environmental Quality 9:54–60.

Suchet, P. A., J. L. Probst, and W. Ludwig. 2003. Worldwide distribution of continental rock lithology: Implications for the atmospheric/soil CO_2 uptake by continental weathering and alkalinity river transport to the oceans. Global Biogeochemical Cycles 17:1038.

Vitousek, P. M., J. D. Aber, R. W. Howarth, G. E. Likens, P. A. Matson, D. W. Schindler, W. H. Schlesinger, and D. Tilman. 1997. Human alteration of the global nitrogen cycle: sources and consequences. Ecological Applications 7:737–750.

Vitousek, P., O. Chadwick, P. Matson, S. Allison, L. Derry, L. Kettley, A. Luers, E. Mecking, V. Monastra, and S. Porder. 2003. Erosion and the rejuvenation of weathering-derived nutrient supply in an old tropical landscape. Ecosystems 6:762–772.

Walker, T. W., and J. K. Syers. 1976. Fate of phosphorus during pedogenesis. Geoderma 15:1–19.

Wallander, H. 2000. Use of strontium isotopes and foliar K content to estimate weathering of biotite induced by pine seedlings colonised by ectomycorrhizal fungi from two different soils. Plant and Soil 222:215–229.

Weatherburn, M. W. 1967. Phenol-hypochlorite reaction for determination of ammonia. Analytical Chemistry 39:971–974.

Wedepohl, K. H. 1995. The composition of the continental crust. Geochimica et Cosmochimica Acta 59:1217–1232.

West, A. J., A. Galy, and M. Bickle. 2005. Tectonic and climatic controls on silicate weathering. Earth and Planetary Science Letters 235:211–228.

White, A. F., and A. E. Blum. 1995. Effects of climate on chemical-weathering in watersheds. Geochimica et Cosmochimica Acta 59:1729–1747.

Supporting Information

Additional supporting information may be found in the online version of this article at http://onlinelibrary.wiley.com/doi/10.1890/15-0501.1/suppinfo